

Exact calculation of three-body contact interaction to second order¹

N. Kaiser

Physik Department T39, Technische Universität München, D-85747 Garching, Germany

email: nkaiser@ph.tum.de

Abstract

For a system of fermions with a three-body contact interaction the second-order contributions to the energy per particle $\bar{E}(k_f)$ are calculated exactly. The three-particle scattering amplitude in the medium is derived in closed analytical form from the corresponding two-loop rescattering diagram. We compare the (genuine) second-order three-body contribution to $\bar{E}(k_f) \sim k_f^{10}$ with the second-order term due to the density-dependent effective two-body interaction, and find that the latter term dominates. The results of the present study are of interest for nuclear many-body calculations where chiral three-nucleon forces are treated beyond leading order via a density-dependent effective two-body interaction.

PACS: 12.38.Bx, 21.30.Fe, 24.10.Cn

1 Introduction and summary

Recent advances in the formulation and construction of (low-momentum) nuclear interactions in chiral effective field theory have unambiguously revealed the important role played by three-nucleon forces [1, 2, 3]. Three-body forces turn out to be an indispensable ingredient in accurate calculations of few-nucleon systems [4] as well as for the structure of light nuclei [5]. In chiral perturbation theory the three-nucleon interaction can be constructed systematically and consistently together with the nucleon-nucleon potential [1, 2]. At leading order it consists of a zero-range contact-term, a mid-range 1π -exchange component and a long-range 2π -exchange component, where the parameters of the latter component occur also in the (subleading) 2π -exchange NN-potential. The calculation of the subleading chiral three-nucleon force, built up from many pion-loop diagrams etc., has been completed recently in ref.[6] and applications to few-nucleon systems are underway.

Furthermore, it has been demonstrated that by employing low-momentum two-body interactions (instead of traditional hard-core NN-potentials) the nuclear many-body problem becomes significantly more perturbative [7]. This desired simplification is accompanied by a prominent role of the three-nucleon interaction, such that its inclusion is essential in order to achieve (reasonable) saturation of nuclear matter already at the Hartree-Fock level.² The combined repulsive three-body effects counterbalance with increasing density the purely attractive contributions provided by the low-momentum two-body interactions alone. Improved calculations of nuclear matter which aim at reproducing the empirical saturation point, $\bar{E}_0 \simeq -16$ MeV, $\rho_0 \simeq 0.16$ fm⁻³, still have to treat second-order (and even higher-order) corrections which arise

¹Work supported in part by BMBF, GSI and the DFG cluster of excellence: Origin and Structure of the Universe.

²At this point it should be noted that three-nucleon forces are unavoidable, independently of whether one uses low-momentum or conventional NN-potentials for nuclear matter calculations. Hard-core NN-potentials are simply not usable in perturbative many-body calculations and one has to treat them at least at the Brueckner-Hartree-Fock level.

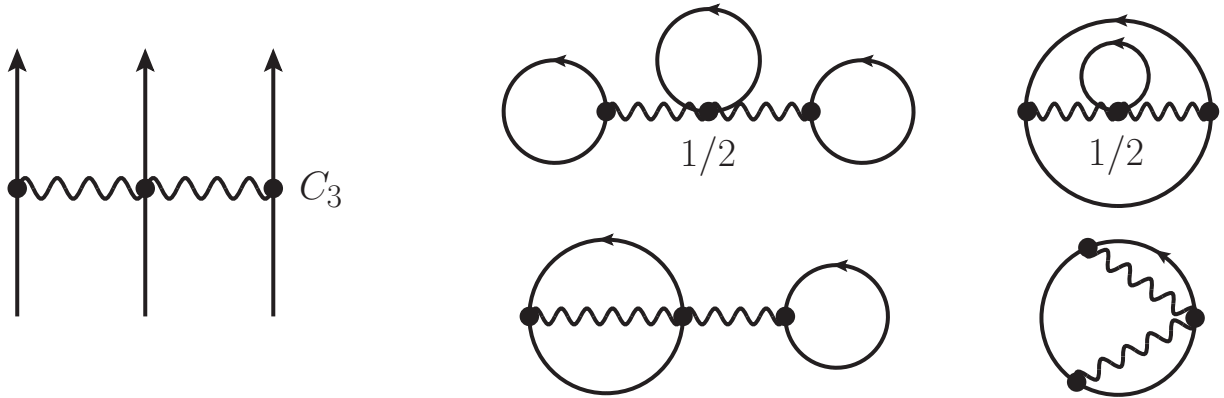


Figure 1: Left: Three-body contact coupling modelled by heavy scalar-isoscalar boson exchange. Right: Closed three-loop diagrams representing the energy density linear in C_3 .

in many-body perturbation theory from the low-momentum two- and three-nucleon interactions [8]. An approximate treatment at second order (and beyond) is commonly pursued by mapping the three-nucleon force onto a density-dependent effective two-body interaction. The detailed form of the density-dependent effective NN-interaction as it results from the leading order chiral three-nucleon interaction has been worked in ref.[9], in particular with regard to its implementation into nuclear structure calculations.

The present paper aims to overcome this common approximation by performing an exact second-order calculation for the simplest three-body interaction, namely for the zero-range contact interaction. Our paper is organized as follows. In section 2 we recapitulate the first order calculation of the energy per particle $\bar{E}(k_f) \sim k_f^6$ and outline different methods to compute the spin-isospin weight factors of closed three-body diagrams. In section 3 the two-loop diagram describing the three-particle rescattering in the medium is evaluated in detail. Analytical expressions are derived for the corresponding vacuum term B_0 , and for the medium corrections B_1 and B_2 incorporating Pauli-blocking effects due to one and two particles, respectively. The ultraviolet divergence in the vacuum loop B_0 requires the introduction of a (Galilei-invariant) three-body counterterm proportional to fourth powers of momenta. The analytical results for $B_{0,1,2}$ are then used in section 4 to compute the second-order (i.e. five-loop) contribution to the energy per particle $\bar{E}(k_f) \sim k_f^{10}$. By comparing this novel result with the second-order term provided by the density-dependent effective two-body interaction, one deduces from the numerical prefactors that the latter term actually dominates (by about a factor 2). The appendix contains two remarkable reduction formulas for special integrals over the product of three Fermi spheres.

The present result obtained in an exact second-order calculation with a simple three-body contact interaction may serve to support the approximate treatment of chiral three-nucleon forces in nuclear matter calculations [7, 8]. Nevertheless, complete second-order calculations with the finite-range chiral three-nucleon forces should be attempted in the future.

2 First order calculation and weight factors

We start out with reproducing the first order calculation of the energy per particle $\bar{E}(k_f)$ from a three-body contact interaction. This allows us to fix the notation for the coupling constant and to discuss alternative methods for computing the spin-isospin weight factors of closed three-body diagrams. The involved combinatorics becomes most transparent if one models the contact-vertex C_3 by the exchange of two heavy scalar-isoscalar bosons. The topologically distinct

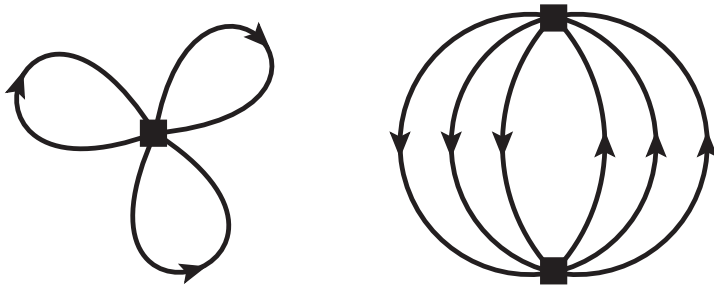


Figure 2: First and second order diagrams generated by a three-body contact interaction.

diagrams obtained by closing all three nucleon lines are shown in Fig. 1 (together with symmetry factors $1/2$). The resulting spin-isospin weight factor in this approach is $4^3/2 - 4^2 - 4^2/2 + 4 = 12$, and hence the first order contribution to the energy per particle reads:

$$\bar{E}(k_f) = -C_3 \frac{3\pi^2}{2k_f^3} \left(\frac{k_f^3}{6\pi^2} \right)^3 \cdot 12 = -\frac{C_3 k_f^6}{12\pi^4} = \Gamma_3 k_f^6, \quad (1)$$

with the density given by $\rho = 2k_f^3/3\pi^2$. The factor $k_f^3/6\pi^2$ stems from the volume of a Fermi sphere. For orientation and comparison we note that the coupling constant of the contact-term in the chiral three-nucleon force [1] is parameterized as $C_3 = c_E/f_\pi^4 \Lambda_\chi$. The reduced coupling constant $\Gamma_3 = -C_3/12\pi^4$ is particularly useful to write down compactly the second order contributions (see eqs.(14,16)).

An alternative derivation of the spin-isospin weight factors starts from a contact-vertex that additionally includes the three-particle antisymmetrization operator:

$$\mathcal{A} = \sum_{\alpha \in S_3} \text{sign}(\alpha) \mathcal{P}_\alpha[\boldsymbol{\sigma}\boldsymbol{\tau}] = (\mathbf{1} - \mathcal{P}_{12})(\mathbf{1} - \mathcal{P}_{13} - \mathcal{P}_{23}). \quad (2)$$

Here, $\mathcal{P}_{ij} = (\mathbf{1} + \vec{\sigma}_i \cdot \vec{\sigma}_j)(\mathbf{1} + \vec{\tau}_i \cdot \vec{\tau}_j)/4$ is the exchange operator for particles i and j , operating in their respective spin and isospin spaces. For the first order three-body diagram (shown in the left part of Fig. 2) a trace has to be taken over the spin- and isospin degrees of freedom of all three nucleons, leading to the result:

$$\frac{3C_3}{6} \text{Tr} \mathcal{A} = \frac{C_3}{2} 64 \left(1 - \frac{1}{4} - \frac{1}{4} - \frac{1}{4} + \frac{1}{16} + \frac{1}{16} \right) = \frac{C_3}{2} 64 \cdot \frac{3}{8} = 12C_3. \quad (3)$$

Here, the symmetry factor $1/6$ accounts for the permutations of the three (indistinguishable) closed nucleon lines and we have displayed separately the contributions from all six permutations $\alpha \in S_3$. The effective coupling constant is now $3C_3$, since in this completely symmetric formulation of the contact-vertex each of the three incoming particles must be joined to the central vertex of the boson-exchange picture in Fig. 1. More interesting is the spin-isospin weight factor of the second order diagram shown in the right part of Fig. 2. Taking into account its symmetry factor $1/6^2$, one gets:

$$\frac{(3C_3)^2}{6^2} \text{Tr} \mathcal{A}^2 = \frac{C_3^2}{4} \text{Tr} 6\mathcal{A} = 36C_3^2 = 12C_3 \cdot 3C_3, \quad (4)$$

where the relation $\mathcal{A}^2 = 6\mathcal{A}$ has been used. The factorization at the end of eq.(4) shows that the three-particle rescattering process carries the relative weight factor $3C_3$.

We finish this section by considering the density-dependent effective two-body interaction which results from closing one nucleon line of the three-body contact-vertex (see Fig. 3). The

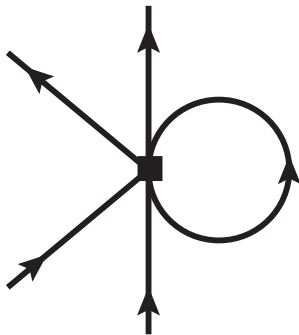


Figure 3: Density-dependent effective 2-body interaction obtained by closing one nucleon line.

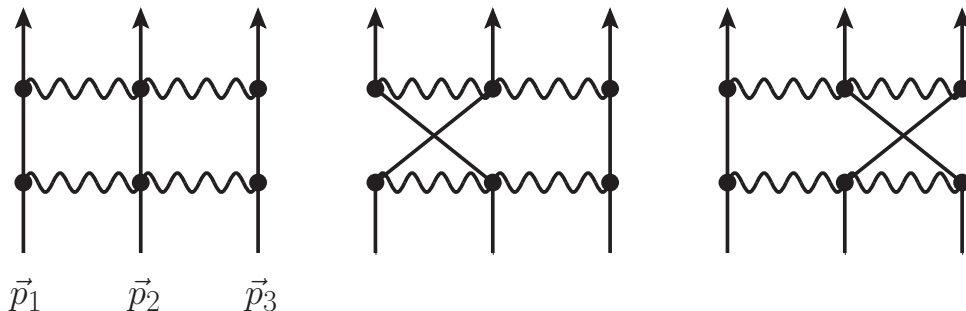


Figure 4: Two-loop diagrams describing the three-particle rescattering in the medium.

method of employing the boson exchange picture gives for the two-body coupling strength:

$$\delta C_0(\rho) = C_3 \left(\frac{k_f^3}{6\pi^2} \right) \cdot 6 = \frac{C_3 k_f^3}{\pi^2}, \quad (5)$$

where the factor $6 = 4 + 4 \cdot 2 - 4 - 2$ emerges from the set of 9 topologically distinct diagrams. Of course, the same result is obtained by including the (two-particle) antisymmetrization operator:

$$\delta C_0(\rho)(\mathbf{1} - \mathcal{P}_{12}) = 3C_3 \left(\frac{k_f^3}{6\pi^2} \right) \text{tr}_3 \mathcal{A} = \frac{C_3 k_f^3}{\pi^2} (\mathbf{1} - \mathcal{P}_{12}), \quad (6)$$

where tr_3 sums over the spin and isospin degrees of freedom of the third nucleon. Having the expression for the effective two-body coupling, $\delta C_0(\rho) = C_3 k_f^3 / \pi^2$, one can immediately give the result for its second order contribution to the energy per particle (see eq.(16)).

3 Three-particle rescattering in the medium

The calculation of the second-order (five-loop) diagram in Fig. 2 proceeds via the three-particle scattering amplitude. The two-loop diagrams describing the three-particle rescattering in the medium are shown in Fig. 4. By including the topologically distinct diagrams with crossings of internal lines the crucial factor 3 deduced in eq.(4) gets accounted for. Each internal line introduces a particle propagator, $i[1 - \theta(k_f - |\vec{l}_j|)] / (l_{0j} - \vec{l}_j^2 / 2M + i\epsilon)$, and after performing the energy integrals via residue calculus the expression for the in-medium scattering amplitude takes the form:

$$B = \int \frac{d^3 l_1 d^3 l_2}{(2\pi)^6} \frac{3C_3 M}{\vec{l}_1^2 + 3\vec{l}_2^2 / 4 - H/6 - i\epsilon} \left[1 - \theta(k_f - |\vec{p} + \vec{l}_1 - \vec{l}_2 / 2|) \right] \\ \times \left[1 - \theta(k_f - |\vec{p} + \vec{l}_2|) \right] \left[1 - \theta(k_f - |\vec{p} - \vec{l}_1 - \vec{l}_2 / 2|) \right]. \quad (7)$$

The chosen assignment of intermediate momenta: $\vec{p} + \vec{l}_1 - \vec{l}_2/2$, $\vec{p} + \vec{l}_2$, $\vec{p} - \vec{l}_1 - \vec{l}_2/2$, with $\vec{p} = (\vec{p}_1 + \vec{p}_2 + \vec{p}_3)/3$, has the advantage that interference terms of the loop momenta $\vec{l}_{1,2}$ among themselves and with the external momenta \vec{p}_j are absent in the energy denominator. The external momenta are to be taken from the region inside the Fermi sphere $|\vec{p}_j| < k_f$, hence the dimensionless variable $s = |\vec{p}|/k_f$ satisfies the condition $0 < s < 1$. The other kinematical quantity H appearing in the energy denominator is the Galileian invariant:

$$H = (\vec{p}_1 - \vec{p}_2)^2 + (\vec{p}_1 - \vec{p}_3)^2 + (\vec{p}_2 - \vec{p}_3)^2 < 9k_f^2. \quad (8)$$

The maximum value $9k_f^2$ of H is reached in the configuration where $\vec{p}_{1,2,3}$ point from the center to the vertices of an equilateral triangle of side-length $\sqrt{3}k_f$. The in-medium scattering amplitude B is manifestly real-valued, since Pauli-blocking and energy conservation forbid any imaginary part: $3k_f^2 < |\vec{p} + \vec{l}_2|^2 + |\vec{p} + \vec{l}_1 - \vec{l}_2/2|^2 + |\vec{p} - \vec{l}_1 - \vec{l}_2/2|^2 = (2\vec{l}_1^2 + 3\vec{l}_2^2/2 - H/3) + \vec{p}_1^2 + \vec{p}_2^2 + \vec{p}_3^2 = \vec{p}_1^2 + \vec{p}_2^2 + \vec{p}_3^2 < 3k_f^2$, where the term in brackets vanishes on-shell.

In the next step one expands the product of the three $(1 - \theta)$ -factors in eq.(7). This rearrangement gives a vacuum part B_0 with no θ -factor, the sum B_1 of three equal terms with one θ -factor, and the sum B_2 of three equal terms with two θ -factors. The equality of the three summands is obvious from the structure of the two-loop diagram and can be shown explicitly by making the substitution $\vec{l}_1 = \sqrt{3}\vec{l}_3/2$. The intermediate momenta are then linear combinations of \vec{l}_2 and \vec{l}_3 with coefficients given by rotations about angles $\pm 2\pi/3$, and the energy denominator $3(\vec{l}_2^2 + \vec{l}_3^2)/4 - H/6$ is clearly invariant under these discrete rotations. At last, there is a contribution B_3 involving three θ -factors. Fortunately, one does not need to evaluate the complicated term $\text{Re } B_3$, because its contribution to the energy per particle $\bar{E}(k_f)$ vanishes identically. The corresponding integral over six Fermi spheres is symmetric under the interchange of the external and internal momenta, except for the energy denominator which changes its sign. To be precise, the denominator in eq.(7) is interpreted in this argument as a principal value.

Next, we have to evaluate the two-loop integrals for B_0 , B_1 and B_2 . The divergent vacuum loop B_0 is treated by dimensional regularization. The three-dimensional integrals in eq.(7) are continued to d dimensions by the rule: $(2\pi)^{-3} \int d^3l_j \rightarrow \lambda^{3-d} (2\pi)^{-d} \int d^d l_j$, which introduces a scale λ in order to preserve mass dimension of the loop integrals. The divergent behavior of the vacuum loop B_0 shows up through an Euler Gamma-function $\Gamma(1 - d)$ and after expanding around $d = 3$ one gets:

$$B_0 = \frac{\sqrt{3}C_3MH^2}{(12\pi)^3} \left\{ \left[\frac{1}{3-d} - \gamma_E + \ln 4\pi \right] + \frac{3}{2}(1 + \ln 3) - \ln \frac{-H - i\epsilon}{\lambda^2} \right\}. \quad (9)$$

A three-body counterterm proportional to H^2 (i.e. fourth power of momenta) is needed to renormalize the three-particle scattering amplitude in vacuum. This is different to the case of two-body scattering, where the vacuum divergence (not visible in dimensional regularization) can be absorbed on the scattering length [10, 11]. It is convenient to introduce via the relation $H = 9k_f^2h$ a second dimensionless variable h , which satisfies together with $s = |\vec{p}|/k_f$ the constraint $s^2 + h < 1$. Using this variable the real part of the renormalized vacuum loop reads:

$$\text{Re } B_0^{(\text{ren})} = \frac{3\sqrt{3}C_3Mk_f^4}{(4\pi)^3} h^2 \left\{ \frac{1}{2}(3 - \ln 3) - 2 \ln \frac{k_f}{\lambda} - \ln h + \text{ct}(\lambda) \right\}, \quad (10)$$

with $\text{ct}(\lambda)$ a parameter for the scale-dependent counterterm.

In order to evaluate the two-loop integral B_1 we select the step-function $\theta(k_f - |\vec{p} + \vec{l}_2|)$. In dimensional regularization the \vec{l}_1 -integral is finite and proportional to $\sqrt{9\vec{l}_2^2 - 2H}$. The

remaining integral over a shifted Fermi sphere of radius k_f leads to the following result for the real part of B_1 :

$$\begin{aligned} \text{Re } B_1 = & \frac{3\sqrt{3}C_3Mk_f^4}{(4\pi)^3} \left\{ \theta((1+s)^2 - 2h) \left[\frac{\sqrt{(1+s)^2 - 2h}}{10s} [16h^2 + h(9s^2 - 7s - 16)] \right. \right. \\ & \left. \left. + (1+s)^3(4-s) \right] - 3h^2 \ln \frac{1+s + \sqrt{(1+s)^2 - 2h}}{\sqrt{2h}} \right] + (s \rightarrow -s) \left. \right\}. \end{aligned} \quad (11)$$

For the evaluation of B_2 we choose the product $\theta(k_f - |\vec{p} + \vec{l}_1 - \vec{l}_2/2|) \theta(k_f - |\vec{p} - \vec{l}_1 - \vec{l}_2/2|)$ of two step-functions. The integral over \vec{l}_1 -space leads to the familiar hole-hole bubble [10, 11] involving several logarithms. The condition for it not to vanish is $|\vec{p} - \vec{l}_2/2| < k_f$ and consequently the integration region in \vec{l}_2 -space is a shifted Fermi sphere of radius $2k_f$. In order to get a more concise representation of B_2 we introduce the following auxiliary function:

$$\begin{aligned} \mathbf{A}(Q, N) &= 2\sqrt{Q} \arctan \frac{N}{\sqrt{Q}}, \quad \text{for } Q > 0, \\ \mathbf{A}(Q, N) &= \sqrt{-Q} \ln \frac{|N + \sqrt{-Q}|}{|N - \sqrt{-Q}|}, \quad \text{for } Q < 0. \end{aligned} \quad (12)$$

The final result for the real-part of B_2 written in terms of the variables s and h has the form:

$$\begin{aligned} \text{Re } B_2 = & \frac{9C_3Mk_f^4}{(4\pi)^4} \left\{ \frac{28}{5}(3-s^2) - \frac{22h}{5} + \left[h(7-15s^2) - 3h^2 - 5 + 10s^2 - \frac{33s^4}{5} \right] \right. \\ & \times \ln \left| 2s^2 - h + \frac{2}{3} \right| + \left[h^2 \left(3 + \frac{1}{2s} \right) + h \left(15s^2 + 7s - 7 - \frac{5}{3s} \right) \right. \\ & \left. + \frac{33s^4}{5} + 2s^3 - 10s^2 - \frac{8s}{3} + 5 + \frac{86}{45s} \right] \ln |2(1+s)^2 - h| \\ & + \frac{16}{45s} (2-3h-3s^2)^2 \left[\mathbf{A}(2-3h-3s^2, 2+3s) - \mathbf{A}(2-3h-3s^2, 3s) \right] \\ & + \frac{1}{10s} \left[2h(13+s-12s^2) - 21h^2 + 2(1+s)^3(3s-2) \right] \\ & \times \left[\mathbf{A}(3(1+s)^2 - 6h, 3(1+s)) - \mathbf{A}(3(1+s)^2 - 6h, 3s-1) \right] \\ & \left. + \frac{64}{3s} \int_0^1 dx x [2(s-x)^2 - h] \mathbf{A} \left(3(s-x)^2 - \frac{3h}{2}, 1-x \right) + (s \rightarrow -s) \right\}. \end{aligned} \quad (13)$$

Note that the symmetrization prescription $+(s \rightarrow -s)$ applies to all terms in the curly brackets, also the first few which are already even functions of s . We remark again that individual components B_j of the three-particle in-medium scattering amplitude possess an imaginary part, but these add up to zero: $\text{Im}(B_0 + B_1 + B_2 + B_3) = 0$.

4 Results: Energy per particle at five-loop order

Having available the analytical expressions for $\text{Re } B_{0,1,2}$ in eqs.(10-13) it is straightforward to compute the second order contribution to the energy per particle $\bar{E}(k_f)$. The pertinent integral over three Fermi spheres (suitably parameterized by three radii and three angles) can be solved in closed form for the polynomial H^2 . Extracting the coefficient of this piece, the expression for the energy per particle at five-loop order (see right diagram in Fig. 2) reads:

$$\bar{E}(k_f) = \frac{37\pi}{175} \Gamma_3^2 M k_f^{10} \left\{ \sqrt{3} \ln \frac{k_f}{\lambda_0} + \zeta_0 + \zeta_1 + \zeta_2 \right\} < 0, \quad (14)$$

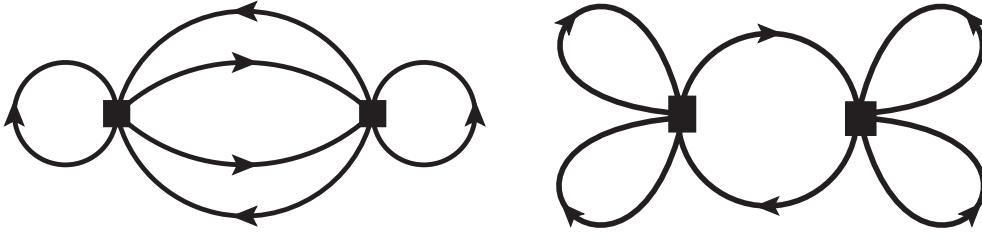


Figure 5: Left: Density-dependent effective two-body interaction to second order. Right: Anomalous three-body diagram which vanishes at zero temperature.

where the counterterm $\text{ct}(\lambda)$ has been absorbed into the logarithm $\ln(k_f/\lambda_0)$. The values of the numerical constants ζ_0 , ζ_1 and ζ_2 as obtained by integrating over three unit spheres are:

$$\zeta_0 = -1.425, \quad \zeta_1 = -5.653, \quad \zeta_2 = -4.354 \pm 0.014, \quad (15)$$

where the errors of ζ_0 and ζ_1 lie beyond the digits given. The result in eq.(14) is to be compared with the second-order contribution from the density-dependent effective two-body interaction as represented by the left diagram in Fig. 5. Converting $\delta C_0(\rho)$ into a scattering length $a(\rho) = C_3 M k_f^3 / 4\pi^3$ and respecting the spin-isospin degeneracy factor $4 - 1 = 3$, one finds from the familiar low-density expansion [10, 11]:

$$\bar{E}(k_f) = \frac{54}{35} \Gamma_3^2 M k_f^{10} (11 - 2 \ln 2) > 0. \quad (16)$$

The numerical factors multiplying $\Gamma_3^2 M k_f^{10}$ in eqs.(16,14) have the values $54(11 - 2 \ln 2)/35 = 14.83$ and $37\pi(\zeta_0 + \zeta_1 + \zeta_2)/175 = -7.59$. Their comparison reveals that the repulsive second order contribution from the density-dependent effective two-body interaction is dominant, but gets reduced to about half of its size by the (genuine) second order three-body contribution. The additional logarithmic term $-1.15 \ln(\lambda_0/k_f)$ does not change this balance in a significant way, assuming that the scale λ_0 is of natural size. For the sake of completeness we note that at five-loop order one can additionally construct the anomalous three-body diagram shown in the right part of Fig. 5. It involves in the central loop the squared in-medium propagator and it vanishes (at zero temperature) by reason of the identity: $\theta(k_f - |\vec{l}|)[1 - \theta(k_f - |\vec{l}|)] = 0$.

The expressions in eqs.(14,16) for the energy per particle $\bar{E}(k_f) \sim \Gamma_3^2 M k_f^{10}$ at five-loop order constitute the main results of the present work. These analytical results demonstrate that by treating a three-body (contact) interaction through the density-dependent two-body interaction only [7, 8] second order effects in many-body perturbation get considerably overestimated. Clearly, after having made this observation in a special case one should attempt complete second-order calculations with the finite-range chiral three-nucleon forces in the future.

Appendix: Reduction formulas for integrals over three Fermi spheres

In this appendix we present two remarkable reduction formulas for integrals over the product of three Fermi spheres. In the first case we assume a dependence of the integrand on the symmetric variable $s = |\vec{p}_1 + \vec{p}_2 + \vec{p}_3|/3k_f$. The following reduction formula holds:

$$\int_{|\vec{p}_j| < k_f} \frac{d^3 p_1 d^3 p_2 d^3 p_3}{(2\pi)^9} F\left(\frac{|\vec{p}_1 + \vec{p}_2 + \vec{p}_3|}{3k_f}\right) = \frac{9k_f^9}{280(2\pi)^6} \int_0^1 ds w(s) F(s), \quad (17)$$

with the (non-smooth) weighting function:

$$w(s) = 27s(1-s)^4(9s^3 + 36s^2 + 27s - 2) + \theta(1-3s) s(1-3s)^4(54 + 53s - 12s^2 - 9s^3). \quad (18)$$

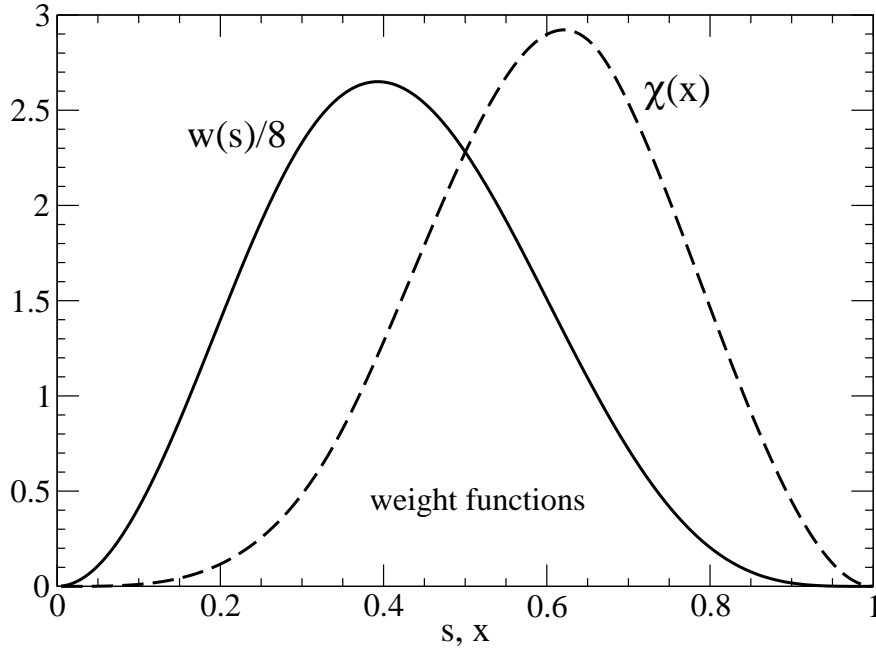


Figure 6: Weight functions $w(s)/8$ and $\chi(x)$. The area under both curves is equal to $280/243$.

This peculiar result for $w(s)$ has been obtained with the help of Fourier transformation techniques and eq.(17) has been checked numerically for many examples of $F(s)$.

In the second case we assume a dependence of the integrand on the combination $s^2 + h = (\vec{p}_1^2 + \vec{p}_2^2 + \vec{p}_3^2)/3k_f^2$ and derive the following reduction formula:

$$\int_{|\vec{p}_j| < k_f} \frac{d^3 p_1 d^3 p_2 d^3 p_3}{(2\pi)^9} G\left(\frac{\vec{p}_1^2 + \vec{p}_2^2 + \vec{p}_3^2}{3k_f^2}\right) = \frac{9k_f^9}{35(2\pi)^6} \int_0^1 dx \chi(x) G(x), \quad (19)$$

with the (non-smooth) weighting function

$$\begin{aligned} \chi(x) = & 6\pi x^3 \sqrt{3x} + \theta(3x-1) \pi \left[\frac{1}{4}(5-42x+105x^2) - 18x^3 \sqrt{3x} \right] \\ & + \theta(3x-2) \left\{ 12x^3 \sqrt{3x} \arccos \frac{1+18x-27x^2}{(3x-1)^3} + 3\sqrt{3x-2} \right. \\ & \left. \times (5-9x+4x^2) + (42x-5-105x^2) \arctan \sqrt{3x-2} \right\}. \end{aligned} \quad (20)$$

This intricate expression for $\chi(x)$ has been obtained by inverting the order of integrations over the three involved radial coordinates $p_j^2/3k_f^2$, while fixing their sum to x . Numerical checks of eq.(19) have been performed for many examples of $G(x)$ as well.

Fig. 6 shows the two weight functions $w(s)/8$ and $\chi(x)$ next to each other. The area under both (bell-shaped) curves is equal to $280/243 = 1.152$. A quick analysis gives that $w(s)/8$ reaches its maximum value of 2.65 at $s = 0.393$, while $\chi(x)$ reaches its maximum value of 2.92 at $x = 0.621$. The behavior at the kinematical endpoints is opposite: $w(s) = 350s^2$, $s \rightarrow 0$ and $w(s) = 1890(1-s)^4$, $s \rightarrow 1$ versus $\chi(x) = 6\pi\sqrt{3}x^{7/2}$, $x \rightarrow 0$ and $\chi(x) = 105(1-x)^2/2$, $x \rightarrow 1$.

Acknowledgement

I thank J.W. Holt for informative discussions.

References

- [1] E. Epelbaum, *Prog. Part. Nucl. Phys.* **57**, 654 (2006); and refs. therein.
- [2] E. Epelbaum, H.-W. Hammer and Ulf-G. Meißner, *Rev. Mod. Phys.* **81**, 1773 (2009).
- [3] S.K. Bogner, R.J. Furnstahl and A. Schwenk, *Prog. Part. Nucl. Phys.* **65**, 94 (2010).
- [4] A. Nogga, S.K. Bogner and A. Schwenk, *Phys. Rev.* **C70**, 061002 (2004).
- [5] P. Navratil et al., *Phys. Rev. Lett.* **99**, 042501 (2007).
- [6] V. Bernard, E. Epelbaum, H. Krebs and Ulf-G. Meißner, *Phys. Rev.* **C77**, 064004 (2008).
- [7] S.K. Bogner, R.J. Furnstahl, A. Nogga and A. Schwenk, *Nucl. Phys.* **A763**, 59 (2005).
- [8] K. Hebeler et al., *Phys. Rev.* **C83**, 031301 (2011).
- [9] J.W. Holt, N. Kaiser and W. Weise, *Phys. Rev.* **C81**, 024002 (2010).
- [10] T. Schäfer, C.W. Cao and S.R. Cotanch, *Nucl. Phys.* **A762**, 82 (2005).
- [11] N. Kaiser, *Nucl. Phys.* **A860**, 41 (2011).